

## QCD corrections to scalar quark pair production in $e^+e^-$ annihilation

A. ARHRIB\*, M. CAPDEQUI-PEYRANERE

Physique Mathématique et Théorique, U.R.A. 768 du CNRS,  
Université de Montpellier II, 34095 Montpellier Cedex 5, France

and

A. DJOUADI

Groupe de Physique des Particules, Université de Montréal,  
Case 6128A, H3C 3J7 Montréal PQ, Canada

### Abstract

We calculate the QCD radiative corrections to the production of the supersymmetric scalar partners of quarks in  $e^+e^-$  annihilation. We include both the standard gluonic corrections and the genuine supersymmetric QCD corrections due to quark-gluino loops, and allow for mixing between left- and right-handed scalar quarks which leads to the possibility that the two final state particles have different masses. The corrections are found to be much larger than the ones affecting the production of spin  $\frac{1}{2}$  particles.

---

\*Also at Université Cadi Ayyad, Faculté des Sciences-Semlalia, L.P.T.N, B.P. S15 Marrakech, Maroc.

# 1. Introduction

One of the best motivated extensions of the Standard Model (SM) of the strong, electromagnetic and weak interactions is Supersymmetry (SUSY); for reviews see Refs. [1, 2]. Supersymmetric theories provide an elegant way to stabilize [3] the huge hierarchy between the electroweak symmetry breaking scale and the Grand Unification or Planck scales against radiative corrections, and its minimal version, the minimal supersymmetric Standard Model (MSSM), allows for a consistent unification of the gauge coupling constants, in contrast to the nonsupersymmetric SM [4]; moreover it offers a natural solution of the cosmological Dark Matter problem [5].

The MSSM predicts the existence of scalar partners to all known quarks and leptons. Since SUSY is broken, these particles can have masses much larger than the masses of their standard partners; however, naturalness arguments suggest that the scale of SUSY breaking, and hence the masses of the SUSY particles, should not exceed  $\mathcal{O}(1 \text{ TeV})$ . So far, the search for SUSY particles at colliders has not been successful and under some assumptions, one can only set lower limits of  $\mathcal{O}(100 \text{ GeV})$  for squarks [6] and below  $\sim 50 \text{ GeV}$  for sleptons [7] on their masses. Higher energy hadron and  $e^+e^-$  colliders will be required to sweep the entire mass range, up to  $\mathcal{O}(1 \text{ TeV})$ , for the SUSY particles.

For a precise prediction of the the production rates of these particles, radiative corrections [at least those which are expected to be rather large] should be incorporated. In particular, because the strong coupling constant is large, the QCD corrections to squark pair production must be included. The QCD corrections to squark pair production at proton colliders have been derived recently [8]. At  $e^+e^-$  colliders, part of the QCD corrections to squark pair production [the ones due to virtual gluon exchange and real gluon emission in the case where the squarks have equal mass] can be adapted from a result obtained long time ago by Schwinger [9] in scalar QED; see also Ref. [10]. However, in the MSSM, this result is not complete for two reasons. First, it is well known that the SUSY partners of left-handed and right-handed massive quarks mix [11] and the mixing will allow for the two mass eigenstates to be non-degenerate; therefore, the Schwinger result must be generalized to allow for the possibility that the final state squarks have different masses. Second, in SUSY theories, the gluons have also spin  $\frac{1}{2}$  partners, the gluinos, which interact strongly with squarks and quarks; the gluino-quark-squark interaction will induce a new type of QCD corrections which has also to be included.

It is the purpose of this paper to provide the complete result for the QCD corrections to squark pair production in  $e^+e^-$  annihilation, allowing for the possibility of having two squarks with different masses in the final state, and including both the standard gluonic corrections and the corrections due to quark-gluino loops.

The paper is organized as follows. In the next section, we will first set the notation and exhibit the various couplings as well as the tree-level results which will be relevant to our discussion. In section 3 and 4, we will give the analytical results for the standard gluonic corrections and for the corrections due to quark-gluino loops respectively; results for the equal mass case will also be given explicitly. In section 5, we will discuss the magnitude of these

QCD effects. A short conclusion is given in section 6. For completeness, we will list in the Appendix the scalar one, two and three–point functions which appear in our results.

## 2. Notation and tree–level results

The production of squark pairs in  $e^+e^-$  collisions proceeds through  $s$ –channel photon and  $Z$  boson exchanges. The interaction of a neutral gauge boson  $V = \gamma, Z$  with squark current eigenstates are described by the following lagrangian [1]:

$$\mathcal{L}_{\tilde{q}\tilde{q}V} = -ieA^\mu \sum_{i=L,R} e_q \tilde{q}_i^* \overleftrightarrow{\partial}_\mu \tilde{q}_i - \frac{ie}{s_W c_W} Z^\mu \sum_{i=L,R} (I_q^{3L} - e_q s_W^2) \tilde{q}_i^* \overleftrightarrow{\partial}_\mu \tilde{q}_i \quad (2.1)$$

with  $I_q^{3L} = \pm 1/2$  and  $e_q$  the weak isospin and the electric charge [in units of the proton charge  $e$ ] of the squark, respectively;  $s_W^2 = 1 - c_W^2 = \sin^2 \theta_W$ . As previously mentioned, the supersymmetric partners of left– and right–handed massive quarks will mix [11], the mass eigenstates  $\tilde{q}_1$  and  $\tilde{q}_2$  being related to the current eigenstates  $\tilde{q}_L$  and  $\tilde{q}_R$  by

$$\tilde{q}_1 = \tilde{q}_L \cos \tilde{\theta}_q + \tilde{q}_R \sin \tilde{\theta}_q \quad , \quad \tilde{q}_2 = -\tilde{q}_L \sin \tilde{\theta}_q + \tilde{q}_R \cos \tilde{\theta}_q \quad (2.2)$$

The mixing angle  $\tilde{\theta}_q$  is proportional to the mass of the quark  $q$ . In the case of the supersymmetric partners of the light quarks, mixing between the current eigenstates can therefore be neglected. However, mixing between top squarks can be sizeable and allows one of the two mass eigenstates to be much lighter than the top quark. Bottom squark mixing can also be significant if the ratio of the vacuum expectation values of the two Higgs fields which give separately masses to isospin up and isospin down type fermions is very large. After the introduction of this squark mixing, the coupling between a gauge boson  $V$  and two squarks  $\tilde{q}_i$  and  $\tilde{q}_j$  with  $i, j = 1, 2$  are given by [the directions of the momenta are shown in Fig. 1a]

$$\Gamma_{\tilde{q}_i \tilde{q}_j \gamma}^\mu = -ie e_q (k_1 + k_2)^\mu \delta_{ij} \quad , \quad \Gamma_{\tilde{q}_i \tilde{q}_j Z}^\mu = -\frac{ie}{4s_W c_W} (k_1 + k_2)^\mu a_{ij}$$

$$a_{11} = 2(2I_q^{3L} \cos^2 \tilde{\theta}_q - 2s_W^2 e_q) \quad , \quad a_{22} = 2(2I_q^{3L} \sin^2 \tilde{\theta}_q - 2s_W^2 e_q) \quad , \quad a_{12} = a_{21} = -2I_q^{3L} \sin 2\tilde{\theta}_q \quad (2.3)$$

In our convention, the couplings of quarks to the photon and the  $Z$  boson are given by

$$\begin{aligned} \Gamma_{q\bar{q}\gamma}^\mu &= -ie e_q \gamma^\mu \quad , \quad \Gamma_{q\bar{q}Z}^\mu = -\frac{ie}{4s_W c_W} \gamma^\mu (v_q - a_q \gamma_5) \\ v_q &= 2I_q^{3L} - 4s_W^2 e_q \quad , \quad a_q = 2I_q^{3L} \end{aligned} \quad (2.4)$$

When discussing QCD corrections we will also need the squark–squark–gluon and squark–squark–gluon–electroweak gauge boson interaction lagrangians which read [1]

$$\begin{aligned} \mathcal{L}_{g\tilde{q}\tilde{q}} &= -ig_s T^a g_a^\mu [\tilde{q}_1^* \overleftrightarrow{\partial}_\mu \tilde{q}_1 + \tilde{q}_2^* \overleftrightarrow{\partial}_\mu \tilde{q}_2] \\ \mathcal{L}_{\tilde{q}_i \tilde{q}_i gV} &= 2g_s e T^a g_a^\mu \sum_{i=L,R} \left[ e_q A_\mu \tilde{q}_i^* \tilde{q}_i + \frac{1}{c_W s_W} (I_q^{3i} - e_q s_W^2) Z_\mu \tilde{q}_i^* \tilde{q}_i \right] \end{aligned} \quad (2.5)$$

Finally, we need the squark–quark–gluino interaction lagrangian which, in the presence of squark mixing, is given by [12]

$$\mathcal{L}_{\tilde{g}\tilde{q}q} = -i\sqrt{2}g_S T^a \tilde{q} [(\tilde{v}_1 + \tilde{a}_1 \gamma_5)\tilde{q}_1 + (\tilde{v}_2 + \tilde{a}_2 \gamma_5)\tilde{q}_2] \tilde{g}^a + \text{h.c.} \quad (2.6)$$

where  $g_S$  is the strong coupling constant,  $T^a$  are  $SU(3)_C$  generators and  $\tilde{v}_i, \tilde{a}_i$  are given by

$$\tilde{v}_1 = \frac{1}{2}(\cos \tilde{\theta}_q - \sin \tilde{\theta}_q) = \tilde{a}_2 \quad , \quad \tilde{a}_1 = \frac{1}{2}(\cos \tilde{\theta}_q + \sin \tilde{\theta}_q) = -\tilde{v}_2 \quad (2.7)$$

In the Born approximation, the total cross section for the production of a pair of squarks [possibly with different masses when produced through  $s$ -channel  $Z$  boson exchange]  $\tilde{q}_i$  and  $\tilde{q}_j$  in  $e^+e^-$  annihilation, including the finite width of the  $Z$  boson, is given by

$$\sigma^B(e^+e^- \rightarrow \tilde{q}_i\tilde{q}_j) = \frac{\pi\alpha^2}{s} \lambda_{ij}^{3/2} \left[ e_q^2 \delta_{ij} - \frac{e_q v_e a_{ij} \delta_{ij}}{16c_W^2 s_W^2} \frac{s}{s - M_Z^2} + \frac{(a_e^2 + v_e^2) a_{ij}^2}{256s_W^4 c_W^4} \frac{s^2}{(s - M_Z^2)^2 + \Gamma_Z^2 M_Z^2} \right] \quad (2.8)$$

with  $s = q^2 = (k_1 - k_2)^2$  the center of mass energy of the  $e^+e^-$  collider and  $\lambda_{ij}$  the usual two-body phase-space function,

$$\lambda_{ij} = (1 - \mu_i^2 - \mu_j^2)^2 - 4\mu_i^2 \mu_j^2 \quad , \quad \mu_{i,j}^2 = \tilde{m}_{q_{i,j}}^2 / s \quad (2.9)$$

In the case where the mixing between squarks is neglected [as is the case for the supersymmetric partners of light quarks and for stop and sbottom quarks if the parameter which describes the strength of the non-SUSY trilinear scalar interactions  $A_{t,b}$  and the SUSY Higgs(ino) mass which also enters trilinear scalar vertices  $\mu$ , are set to zero] the total cross section for left- and right-handed squark pair production simplifies to [10, 12]

$$\sigma^B(e^+e^- \rightarrow \tilde{q}_i\tilde{q}_i) = \frac{\pi\alpha^2}{s} \beta_q^3 \left[ e_q^2 - \frac{e_q v_e v_{q_i}}{16c_W^2 s_W^2} \frac{s}{s - M_Z^2} + \frac{(a_e^2 + v_e^2) v_{q_i}^2}{256s_W^4 c_W^4} \frac{s^2}{(s - M_Z^2)^2 + \Gamma_Z^2 M_Z^2} \right] \quad (2.10)$$

with

$$v_{\tilde{q}_1} = v_{\tilde{q}_L} = v_q + a_q \quad , \quad v_{\tilde{q}_2} = v_{\tilde{q}_R} = v_q - a_q \quad (2.11)$$

Note that, as it is expected for the production of scalar particles in  $e^+e^-$  annihilation, the cross section is proportional to the third power of the velocity of the final squarks,  $\beta_q = (1 - 4\tilde{m}_q^2/s)^{1/2}$ , and therefore is strongly suppressed near threshold. The angular distribution is also typical for spin-zero particle production, it is given by [ $\theta$  is the scattering angle]

$$\frac{d\sigma^B}{d\cos\theta}(e^+e^- \rightarrow \tilde{q}_i\tilde{q}_j) = \frac{3}{4} \sin^2\theta \sigma^B(e^+e^- \rightarrow \tilde{q}_i\tilde{q}_j) \quad (2.12)$$

In order to include QCD corrections at first order in  $\alpha_S$ , one needs to consider the diagrams in Fig. 1b–1e, the contributions of which will be discussed in the next two sections.

### 3. Gluonic corrections

The first set of  $\mathcal{O}(\alpha_S)$  contributions is due to the standard QCD gluonic corrections. They consist first on the interference between the contribution of the tree-level diagram Fig. 1a and the sum of the vertex correction Fig. 1b and the squark wave function renormalization Fig. 1c, where a gluon is exchanged in the squark legs. These two contributions are separately ultraviolet divergent and these divergences are regulated using the dimensional regularization scheme. The sum of the two contributions is, as it should be, ultraviolet finite but it is infrared divergent; this last divergence is regulated by introducing a fictitious mass  $m_g$  for the gluon. One has also to include the contribution of the bremsstrahlung diagrams where a gluon is emitted from the external squark lines, Fig. 1d. This contribution is also infrared divergent, but the sum of the virtual and real corrections is infrared finite as expected. Summing all corrections, the cross section at  $\mathcal{O}(\alpha_S)$  can be written as

$$\sigma(e^+e^- \rightarrow \tilde{q}_i\tilde{q}_j) = \sigma^B(e^+e^- \rightarrow \tilde{q}_i\tilde{q}_j) \left[ 1 + \frac{4\alpha_S}{3\pi} \Delta_{ij} \right] \quad , \quad \Delta_{ij} = \Delta_{ij}^V + \Delta_{ij}^R \quad (3.1)$$

where  $\Delta_{ij}^V$  corresponds to the contribution of the virtual exchange of gluons and  $\Delta_{ij}^R$  to the contribution of gluon emission from the final state squarks.

#### 3.1 Virtual Corrections

Summing the vertex correction and the squark wave function renormalization contributions, which as previously mentioned are separately ultraviolet divergent, one obtains for the interference between the tree level diagram and the ones of Fig. 1b–1c [after normalizing to the Born term and factorizing out  $4\alpha_S/3\pi$ ]

$$\begin{aligned} \Delta_{ij}^V = & \log \frac{\mu_i\mu_j}{\mu_g^2} - 2 + \frac{1}{\lambda_{ij}^{1/2}}(1 - \mu_i^2 - \mu_j^2) \log \frac{1 - \mu_i^2 - \mu_j^2 + \lambda_{ij}^{1/2}}{1 - \mu_i^2 - \mu_j^2 - \lambda_{ij}^{1/2}} \\ & + \frac{1}{2\lambda_{ij}^{1/2}}(1 - \mu_i^2 - \mu_j^2) \left( \log \frac{1 - \mu_i^2 - \mu_j^2 + \lambda_{ij}^{1/2}}{2\mu_i\mu_j} \log \mu_g^2 + F_{ij}^V \right) \end{aligned} \quad (3.2)$$

with the scaled variable  $\mu_g^2 = m_g^2/s$  where  $m_g$  is a fictitious gluon mass introduced to regularize the infrared divergence. The ultraviolet and infrared finite function  $F_{ij}^V$  is given by

$$\begin{aligned} F_{ij}^V = & \frac{1}{2} [\log^2(1 - y_1) - \log^2(-y_1) - \log^2(1 - y_2) + \log^2(-y_2)] + 2 \log \frac{(1 - y_1)}{(-y_1)} \log(y_1 - y_2) \\ & + \log(-y_1) \log(-y_2) - \log(1 - y_1) \log(1 - y_2) + 2\text{Li}_2 \left( \frac{y_1}{y_1 - y_2} \right) - 2\text{Li}_2 \left( \frac{y_1 - 1}{y_1 - y_2} \right) \end{aligned} \quad (3.3)$$

with  $\text{Li}_2$  the usual Spence function defined as  $\text{Li}_2(x) = -\int_0^1 dt \log(1 - xt)t^{-1}$  and the variables  $y_{1/2}$  given by

$$y_{1/2} = \frac{1}{2}(1 + \mu_i^2 - \mu_j^2 \pm \lambda_{ij}^{1/2}) \quad (3.4)$$

Note that the term in the second line of eq. (3.2) [up to a coefficient  $(1 - \mu_i^2 - \mu_j^2)/s$ ] is just the Passarino–Veltman [13, 14] scalar three–point function in a particular case

$$C_0(k_1^2, k_2^2, s, \tilde{m}_{q_i}, m_g, \tilde{m}_{q_j}) = \frac{1}{2s\lambda_{ij}^{1/2}} \left( 2 \log \frac{1 - \mu_i^2 - \mu_j^2 + \lambda_{ij}^{1/2}}{2\mu_i\mu_j} \log \mu_g + F_{ij}^V \right) \quad (3.5)$$

the general form of which is given in the Appendix.

### 3.2 Real Corrections

In terms of the momenta of the particles in the final state [ $k$  is the four–momentum of the gluon], the amplitude squared of the process  $e^+e^- \rightarrow \tilde{q}_i\tilde{q}_jg$  is given by

$$\begin{aligned} |M|^2(e^+e^- \rightarrow \tilde{q}_i\tilde{q}_jg) &= \frac{4g_S^2e^4}{3s} \left[ e_q^2\delta_{ij} - \frac{e_qv_e a_{ij}\delta_{ij}}{16c_W^2s_W^2} \frac{s}{s - M_Z^2} + \frac{(a_e^2 + v_e^2)a_{ij}^2}{256s_W^4c_W^4} \frac{s^2}{(s - M_Z^2)^2 + \Gamma_Z^2M_Z^2} \right] \\ &\times \left[ 8 - \lambda_{ij} \left( \frac{s^2\mu_i^2}{(k_1 \cdot k)^2} + \frac{s^2\mu_j^2}{(k_2 \cdot k)^2} + \frac{2s}{k_1 \cdot k} + \frac{2s}{k_2 \cdot k} + \frac{s^2(\mu_i^2 + \mu_j^2 - 1)}{(k_1 \cdot k)(k_2 \cdot k)} \right) \right] \quad (3.6) \end{aligned}$$

Note that, as a consequence of gauge invariance, the amplitude for the sum of the three diagrams of Fig. 1d, should vanish when multiplied by the four–momentum of the gluon; this provides a good check of the calculation.

The integrals over the three–body phase space in the general case where the masses of the two squarks are unequal [and where both the soft and hard bremsstrahlung contributions are added up] can be found for instance in Ref. [15]. Again, after normalizing to the Born term and factorizing out  $4\alpha_S/3\pi$ , one obtains for the real corrections  $\Delta_{ij}^R$  with  $i \neq j$

$$\begin{aligned} \Delta_{ij}^R &= \frac{1 - \mu_i^2 - \mu_j^2}{\lambda_{ij}^{1/2}} \left[ 2 \log^2 \lambda_0 - \log^2 \lambda_1 - \log^2 \lambda_2 + 2\text{Li}_2(1 - \lambda_0^2) - \text{Li}_2(1 - \lambda_1^2) - \text{Li}_2(1 - \lambda_2^2) \right] \\ &+ \frac{4}{\lambda_{ij}^{3/2}} \left[ \frac{1}{4} \lambda_{ij}^{1/2} (1 + \mu_i^2 + \mu_j^2) + \mu_i^2 \log \lambda_2 + \mu_j^2 \log \lambda_1 + \mu_i^2 \mu_j^2 \log \lambda_0 \right] + 4 + \frac{1 + 2\mu_j^2}{\lambda_{ij}^{1/2}} \log \lambda_2 \\ &+ \frac{1 + 2\mu_i^2}{\lambda_{ij}^{1/2}} \log \lambda_1 + \left[ \frac{(1 - \mu_i^2 - \mu_j^2)}{\lambda_{ij}^{1/2}} \log \lambda_0 - 1 \right] \log \frac{\lambda_{ij}^2}{\mu_i^2 \mu_j^2} + \frac{(2 + \mu_i^2 + \mu_j^2)}{\lambda_{ij}^{1/2}} \log \lambda_0 \quad (3.7) \end{aligned}$$

with

$$\lambda_0 = \frac{1}{2\mu_i\mu_j} (1 - \mu_i^2 - \mu_j^2 + \lambda_{ij}^{1/2}) \quad , \quad \lambda_{1/2} = \frac{1}{2\mu_{j/i}} (1 \mp \mu_i^2 \pm \mu_j^2 - \lambda_{ij}^{1/2}) \quad (3.8)$$

Note that  $\Delta_{ij}^R$  has the same infrared divergence as  $\Delta_{ij}^V$  but with the opposite sign so that, as it should be, the sum of the two contributions  $\Delta_{ij} = \Delta_{ij}^V + \Delta_{ij}^R$  is infrared finite.

### 3.3 Equal squark mass case

In the case where the two scalar particles in the final state have equal masses, the previous expressions simplify considerably. In terms of the velocity of one of the final squarks one would have for the virtual and real corrections

$$\begin{aligned} \Delta_{ij}^V = & -\log \mu_g^2 \left[ 1 + \frac{1+\beta^2}{2\beta} \log \frac{1-\beta}{1+\beta} \right] - 2 + \log \frac{1-\beta^2}{4} - \frac{1+\beta^2}{\beta} \log \frac{1-\beta}{1+\beta} \\ & + \frac{1+\beta^2}{\beta} \left[ \text{Li}_2 \left( \frac{1-\beta}{1+\beta} \right) + \frac{1}{4} \log^2 \frac{1-\beta}{1+\beta} + \log \beta \log \frac{1-\beta}{1+\beta} + \frac{\pi^2}{3} \right] \end{aligned} \quad (3.9)$$

$$\begin{aligned} \Delta_{ij}^R = & \log \mu_g^2 \left[ 1 + \frac{1+\beta^2}{2\beta} \log \frac{1-\beta}{1+\beta} \right] + \frac{3+7\beta^2}{2\beta^2} + \frac{3-6\beta^2-\beta^4}{4\beta^3} \log \frac{1-\beta}{1+\beta} - 4 \log \beta \\ & + 2 \log \frac{1-\beta^2}{4} + \frac{1+\beta^2}{\beta} \left[ 3\text{Li}_2 \left( \frac{1-\beta}{1+\beta} \right) + 2\text{Li}_2 \left( -\frac{1-\beta}{1+\beta} \right) - \frac{\pi^2}{3} - \frac{5}{4} \log^2 \frac{1-\beta}{1+\beta} \right. \\ & \left. + \log \frac{1-\beta^2}{4\beta^2} \log \frac{1-\beta}{1+\beta} + \log \frac{2\beta}{1+\beta} \log \frac{1-\beta}{1+\beta} + 2 \log \frac{4\beta}{(1+\beta)^2} \log \frac{1-\beta}{1+\beta} \right] \end{aligned} \quad (3.10)$$

Adding these two contributions, one obtains the total gluonic QCD corrections to squark pair production in the equal mass case

$$\begin{aligned} \Delta_{ij} = & \frac{3}{2} \frac{1+\beta^2}{\beta^2} + 3 \log \frac{1-\beta^2}{4} - 4 \log \beta + \frac{3-10\beta^2-5\beta^4}{4\beta^3} \log \frac{1-\beta}{1+\beta} + \frac{1+\beta^2}{\beta} \\ & \times \left[ 4\text{Li}_2 \left( \frac{1-\beta}{1+\beta} \right) + 2\text{Li}_2 \left( -\frac{1-\beta}{1+\beta} \right) + 2 \log \beta \log \frac{1-\beta}{1+\beta} - 3 \log \frac{1+\beta}{2} \log \frac{1-\beta}{1+\beta} \right] \end{aligned} \quad (3.11)$$

This result is in agreement with the one obtained by Schwinger [9] for scalar QED, once a misprint in his eq. (5.4-132) has been corrected; see also Ref. [10].

Let us study the behaviour of this correction in the two limiting situations,  $\beta \rightarrow 1$  or  $0$ . In the limit where the squark mass is much smaller than the center of mass energy,  $\beta \rightarrow 1$ , the QCD correction approaches the value  $\Delta_{ij} \rightarrow 3$ , i.e. it is four times larger than the QCD corrections to the production of massless spin- $\frac{1}{2}$  quarks. In the opposite limit  $\beta \rightarrow 0$ , i.e. for squark masses near the production threshold, one obtains a correction  $\Delta_{ij} \rightarrow \pi^2/(2\beta) - 2$ , which exhibits the well-known Coulomb singularity near threshold; in this case the perturbative analysis is no longer reliable and one has to take into account non-perturbative effects as discussed in Ref. [16].

Finally, let us note that the expression eq. (3.11) can be interpolated by the Schwinger formula [9]

$$\Delta_{ij} \sim \frac{\pi^2}{2\beta} - \frac{1}{4}(1+\beta)(\pi^2 - 6) \quad (3.12)$$

which, up to an error of less than 2%, reproduces the exact result given in eq. (3.11)

## 4. Gluino corrections

Let us now discuss the supersymmetric corrections due to quark–gluino loops. They consist of the vertex correction where the partner quark and a gluino are exchanged, Fig. 1e, and of the contribution of the squark wave function renormalization, Fig. 1f. In the general case where squark mixing is present, leading to two final particles with different masses, the expressions of these contributions are rather complicated.

### 4.1 Vertex Correction

The contribution of the quark–gluino vertex correction to the coupling of the  $Z$  boson to a pair of squarks  $\tilde{q}_i\tilde{q}_j$  can be written as

$$\Gamma_{ij}^\mu = \frac{-ie}{4c_W s_W} \left[ a_{ij} k^\mu + \frac{4}{3} \frac{\alpha_s}{\pi} \delta\Gamma_{ij}^\mu \right] \quad (4.1)$$

where

$$\begin{aligned} \delta\Gamma_{ij}^\mu &= v_q(\tilde{v}_i\tilde{v}_j + \tilde{a}_i\tilde{a}_j) \left\{ q^\mu \left[ (2\tilde{m}_g^2 + 2m_q^2 - \tilde{m}_{q_i}^2 - \tilde{m}_{q_j}^2)C_{ij}^+ + (\tilde{m}_{q_j}^2 - \tilde{m}_{q_i}^2)C_{ij}^- \right] \right. \\ &+ k^\mu \left[ (2\tilde{m}_g^2 + 2m_q^2 + \tilde{m}_{q_i}^2 + \tilde{m}_{q_j}^2)C_{ij}^+ + (\tilde{m}_{q_i}^2 - \tilde{m}_{q_j}^2)C_{ij}^- + 2\tilde{m}_g^2 C_{ij}^0 + B^0(s, m_q^2, m_q^2) \right] \left. \right\} \\ &+ a_q(\tilde{v}_i\tilde{a}_j + \tilde{a}_i\tilde{v}_j) \left\{ q^\mu \left[ (2\tilde{m}_g^2 - 2m_q^2 - \tilde{m}_{q_i}^2 - \tilde{m}_{q_j}^2)C_{ij}^+ + (\tilde{m}_{q_j}^2 - \tilde{m}_{q_i}^2)C_{ij}^- \right] \right. \\ &+ k^\mu \left[ (2\tilde{m}_g^2 - 2m_q^2 + \tilde{m}_{q_i}^2 + \tilde{m}_{q_j}^2)C_{ij}^+ + (\tilde{m}_{q_i}^2 - \tilde{m}_{q_j}^2)C_{ij}^- + 2\tilde{m}_g^2 C_{ij}^0 + B^0(s, m_q^2, m_q^2) \right] \left. \right\} \\ &+ 2\tilde{m}_g m_q q^\mu \left[ 2v_q(\tilde{v}_i\tilde{v}_j - \tilde{a}_i\tilde{a}_j)C_{ij}^- - a_q(\tilde{v}_i\tilde{a}_j - \tilde{a}_i\tilde{v}_j)C_{ij}^0 \right] \\ &+ 2\tilde{m}_g m_q k^\mu v_q(\tilde{v}_i\tilde{v}_j - \tilde{a}_i\tilde{a}_j)(2C_{ij}^+ + C_{ij}^0) \end{aligned} \quad (4.2)$$

where, in terms of the scalar two–point and three point functions  $B^0$  and  $C^0$  which are given in the Appendix, the functions  $C_{ij}^\pm \equiv C^\pm(\tilde{m}_{q_i}^2, \tilde{m}_{q_j}^2, s, m_q, m_q, \tilde{m}_g)$  are given by

$$\begin{aligned} C_{ij}^+ &= -\frac{1}{2s\lambda_{ij}} \left\{ \frac{\tilde{m}_{q_i}^2 - \tilde{m}_{q_j}^2}{s} \left[ B^0(\tilde{m}_{q_i}^2, \tilde{m}_{q_j}^2, m_q^2) - B^0(\tilde{m}_{q_j}^2, \tilde{m}_{q_i}^2, m_q^2) + (\tilde{m}_{q_i}^2 - \tilde{m}_{q_j}^2)C_{ij}^0 \right] \right. \\ &+ B^0(\tilde{m}_{q_i}^2, \tilde{m}_g^2, m_q^2) + B^0(\tilde{m}_{q_j}^2, \tilde{m}_g^2, m_q^2) - 2B^0(s, m_q^2, m_q^2) \\ &\left. + (2m_q^2 - 2\tilde{m}_g^2 - \tilde{m}_{q_i}^2 - \tilde{m}_{q_j}^2)C_{ij}^0 \right\} \end{aligned} \quad (4.3)$$

$$\begin{aligned} C_{ij}^- &= \frac{1}{2s\lambda_{ij}} \left\{ \frac{2\tilde{m}_{q_i}^2 + 2\tilde{m}_{q_j}^2 - s}{s} \left[ B^0(\tilde{m}_{q_i}^2, \tilde{m}_{q_j}^2, m_q^2) - B^0(\tilde{m}_{q_j}^2, \tilde{m}_{q_i}^2, m_q^2) + (\tilde{m}_{q_i}^2 - \tilde{m}_{q_j}^2)C_{ij}^0 \right] \right. \\ &+ \frac{\tilde{m}_{q_i}^2 - \tilde{m}_{q_j}^2}{s} \left[ B^0(\tilde{m}_{q_i}^2, \tilde{m}_g^2, m_q^2) + B^0(\tilde{m}_{q_j}^2, \tilde{m}_g^2, m_q^2) - 2B^0(s, m_q^2, m_q^2) \right. \\ &\left. \left. + (2m_q^2 - 2\tilde{m}_g^2 - \tilde{m}_{q_i}^2 - \tilde{m}_{q_j}^2)C_{ij}^0 \right] \right\} \end{aligned} \quad (4.4)$$



Note that while  $C_{ij}^+$  is symmetric in the interchange of  $\tilde{q}_i$  and  $\tilde{q}_j$ ,  $C_{ij}^-$  is antisymmetric and vanishes in the equal mass case. Note also that only the terms proportional to  $k^\mu = k_1^\mu + k_2^\mu$  are ultraviolet infinite [only the two-point function  $B^0$  is divergent], this has to be expected since the one-loop induced terms proportional to  $q^\mu = k_1^\mu - k_2^\mu$ , which are absent at the tree-level, cannot be renormalized.

The contribution to the coupling of the photon can be straightforwardly derived from the previous expressions by setting to zero the terms proportional to  $a_q$ ; a further simplification is obtained by noting that  $\tilde{v}_1\tilde{v}_2 + \tilde{a}_1\tilde{a}_2 = 0$  and discarding the terms proportional to  $q^\mu$  in the equal mass case [since we are interested in the interference with the Born amplitude, these give rise to  $k \cdot q = \tilde{m}_{q_1}^2 - \tilde{m}_{q_2}^2$  terms which vanish in this case]; one obtains

$$\Gamma_{ij}^\mu = -iee_q \left[ k^\mu \delta_{ij} + \frac{4}{3} \frac{\alpha_s}{\pi} \delta\Gamma_{ij}^\mu \right] \quad (4.5)$$

with

$$\begin{aligned} \delta\Gamma_{ij}^\mu &= k^\mu (\tilde{v}_i\tilde{v}_j + \tilde{a}_i\tilde{a}_j) \left[ (2\tilde{m}_g^2 + 2m_q^2 + \tilde{m}_{q_i}^2 + \tilde{m}_{q_j}^2) C_{ij}^+ + 2\tilde{m}_g^2 C_{ij}^0 + B^0(s, m_q^2, m_q^2) \right] \delta_{ij} \\ &\quad + 2\tilde{m}_g m_q (\tilde{v}_i\tilde{v}_j - \tilde{a}_i\tilde{a}_j) \left[ k^\mu (2C_{ij}^+ + C_{ij}^0) + 2q^\mu C_{ij}^- \right] \end{aligned} \quad (4.6)$$

Note that for  $i \neq j$ , the contribution  $\delta\Gamma_{ij}$  does not vanish alone [because of the terms in the second line of the previous expression: since the two masses  $\tilde{m}_{q_i}$  and  $\tilde{m}_{q_j}$  are not equal, this leads to  $k \cdot q = \tilde{m}_{q_1}^2 - \tilde{m}_{q_2}^2 \neq 0$ ] and this poses the problem of gauge invariance at the photon vertex; however, the left-over piece in the amplitude  $q_\mu \delta\Gamma_{ij}^\mu$

$$q_\mu \delta\Gamma_{ij}^\mu \sim 2(k \cdot q) C_{ij}^+ + (k \cdot q) C_{ij}^0 + 2q^2 C_{ij}^- \rightarrow B^0(\tilde{m}_{q_j}^2, \tilde{m}_g^2, m_q^2) - B^0(\tilde{m}_{q_i}^2, \tilde{m}_g^2, m_q^2) \quad (4.7)$$

is antisymmetric in the interchange of  $i$  and  $j$  so that the sum  $q_\mu \delta\Gamma_{12}^\mu + q_\mu \delta\Gamma_{21}^\mu$ , which enters in the physical process, vanishes and the  $\gamma\tilde{q}_1\tilde{q}_2$  is indeed gauge invariant. This feature provides a good check of the calculation.

## 4.2 Counterterms

One has then to include the renormalization of the squark wave function. In the general case where squark mixing is allowed, this renormalization is a bit more complicated than usual; this is because the wave-functions of the two squarks are not decoupled. In addition one has also to renormalize the mixing angle  $\tilde{\theta}_q$ . Taking into account the mixing, the renormalization of the squark wave functions and the mixing angle  $\tilde{\theta}_q$  can be performed by making the following substitutions in the Lagrangian eq. (2.1)

$$\begin{aligned} \tilde{q}_1 &\rightarrow (1 + \delta Z_{11})^{1/2} \tilde{q}_1 + \delta Z_{12} \tilde{q}_2, & \tilde{q}_2 &\rightarrow (1 + \delta Z_{22})^{1/2} \tilde{q}_2 + \delta Z_{21} \tilde{q}_1 \\ & & \tilde{\theta}_q &\rightarrow \tilde{\theta}_q + \delta\tilde{\theta}_q \end{aligned} \quad (4.8)$$

Under the substitution  $\tilde{\theta}_q \rightarrow \tilde{\theta}_q + \delta\tilde{\theta}_q$ , the couplings  $a_{ij}$  transform as  $a_{ij} \rightarrow a_{ij} + \delta a_{ij}$ , with

$$\delta a_{11} = 2a_{12}\delta\tilde{\theta}_q \quad , \quad \delta a_{22} = -2a_{12}\delta\tilde{\theta}_q \quad , \quad \delta a_{12} = (a_{22} - a_{11})\delta\tilde{\theta}_q \quad (4.9)$$

The full counterterms can then be included by shifting the couplings  $a_{ij}$  in  $\Gamma_{ij}^\mu$  of eq. (4.1) and (4.5) by an amount

$$a_{ij} \rightarrow a_{ij} + \Delta a_{ij} \quad (4.10)$$

with

$$\begin{aligned} \Delta a_{11} &= \delta a_{11} + a_{11}\delta Z_{11} + 2a_{12}\delta Z_{21} \\ \Delta a_{22} &= \delta a_{22} + a_{22}\delta Z_{22} + 2a_{12}\delta Z_{12} \\ \Delta a_{12} &= \delta a_{12} + \frac{1}{2}a_{12}(\delta Z_{11} + \delta Z_{22}) + a_{11}\delta Z_{12} + a_{22}\delta Z_{21} \end{aligned} \quad (4.11)$$

One has then to choose a renormalization condition which defines the mixing angle  $\tilde{\theta}_q$  [and hence  $a_{12}$  through eq. (4.9)]. We choose this condition in such a way that the total quark–gluino QCD correction to the vertex  $Z_\mu\tilde{q}_1\tilde{q}_2$  vanishes at zero–momentum transfer  $q^2 = 0$ ;  $\delta a_{12}$  will be then given by

$$\delta a_{12} = - \left[ \frac{4}{3} \frac{\alpha_S}{\pi} \frac{1}{2} \delta(\Gamma_{12} + \Gamma_{21}) \Big|_{q^2=0} + \frac{1}{2} a_{12} (\delta Z_{11} + \delta Z_{22}) + a_{11} \delta Z_{12} + a_{22} \delta Z_{21} \right] \quad (4.12)$$

In the on–shell scheme, where the renormalized squark propagators are such that their poles are at  $p^2 = \tilde{m}^2$  and the residues at the poles are equal to unity, the counterterms  $\delta Z_{ij}$  read

$$\begin{aligned} \delta Z_{11} &= \Sigma'_{11}(m_{\tilde{q}_1}^2) \quad , \quad \delta Z_{22} = \Sigma'_{22}(m_{\tilde{q}_2}^2) \quad , \\ \delta Z_{12} &= \frac{\Sigma_{12}(m_{\tilde{q}_2}^2)}{m_{\tilde{q}_2}^2 - m_{\tilde{q}_1}^2} \quad , \quad \delta Z_{21} = \frac{\Sigma_{21}(m_{\tilde{q}_1}^2)}{m_{\tilde{q}_1}^2 - m_{\tilde{q}_2}^2} \end{aligned} \quad (4.13)$$

where  $\Sigma_{ij}(m^2)$  and  $\Sigma'_{ii}(m^2) = \partial\Sigma_{ii}(p^2)/\partial p^2|_{p^2=m^2}$  are given by

$$\begin{aligned} \Sigma_{ij}(p^2) &= \frac{4\alpha_S}{3\pi} \left[ (\tilde{v}_i\tilde{v}_j + \tilde{a}_i\tilde{a}_j) [A^0(m_g^2) + A^0(m_q^2) + (m_g^2 + m_q^2 - p^2)B_0(p^2, \tilde{m}_g^2, m_q^2)] \right. \\ &\quad \left. + 2\tilde{m}_g m_q (\tilde{v}_i\tilde{v}_j - \tilde{a}_i\tilde{a}_j) B^0(p^2, \tilde{m}_g^2, m_q^2) \right] \end{aligned} \quad (4.14)$$

and

$$\begin{aligned} \Sigma'_{ii}(p^2) &= -\frac{4\alpha_S}{3\pi} \left[ (\tilde{v}_i^2 + \tilde{a}_i^2) [B_0(p^2, \tilde{m}_g^2, m_q^2) + (p^2 - m_q^2 - \tilde{m}_g^2)B'_0(p^2, \tilde{m}_g^2, m_q^2)] \right. \\ &\quad \left. - 2m_q\tilde{m}_g(\tilde{v}_i^2 - \tilde{a}_i^2)B'_0(p^2, \tilde{m}_g^2, m_q^2) \right] \end{aligned} \quad (4.15)$$

with  $A^0$  and  $B^0$  the scalar one–point and two–point functions which can be found in the Appendix.

### 4.3 Case of vanishing mixing angle

In the case where the mixing angle is set to zero, as is the case for the SUSY partners of the light quarks and for stop and sbottom squarks when  $A_{t,b} = \mu = 0$ , the situation simplifies considerably. One has just to consider separately left- and right-handed squarks, include the vertex correction [with equal squark masses] and the squark wave-function renormalization [with the ones of  $\tilde{q}_1$  and  $\tilde{q}_2$  now decoupled]. The sum of these two contributions is finite and no mixing angle renormalization is needed.

The coupling of the photon and the Z boson to a pair of squarks including the quark-gluino vertex correction and the wave-function renormalization, will read at  $\mathcal{O}(\alpha_S)$

$$\begin{aligned}\Gamma_{\gamma\tilde{q}_i\tilde{q}_i}^\mu &= -iee_q(k_1 + k_2)^\mu \left(1 + \frac{4}{3} \frac{\alpha_S}{\pi} \frac{1}{2} \tilde{\Delta}_{ii}^\gamma\right) \\ \Gamma_{Z\tilde{q}_i\tilde{q}_i}^\mu &= -\frac{ie}{4c_W s_W} (v_q \pm a_q)(k_1 + k_2)^\mu \left(1 + \frac{4}{3} \frac{\alpha_S}{\pi} \frac{1}{2} \tilde{\Delta}_{ii}^Z\right)\end{aligned}\quad (4.16)$$

where in the case of the Z boson, the upper sign is for  $i = 1 = \text{L}$  and the lower sign for  $i = 2 = \text{R}$ ; the corrections factor  $\tilde{\Delta}_{ii}^Z$  is given by

$$\begin{aligned}\tilde{\Delta}_{ii}^Z &= 2 \left[ \tilde{m}_g^2 + \tilde{m}_q^2 + \frac{v_q \mp a_q}{v_q \pm a_q} m_q^2 \right] C_+ + 2\tilde{m}_g^2 C_0 + B_0(s, m_q^2, m_q^2) \\ &\quad - B_0(\tilde{m}_q^2, \tilde{m}_g^2, m_q^2) - (\tilde{m}_q^2 - m_q^2 - \tilde{m}_g^2) B'_0(\tilde{m}_q^2, \tilde{m}_g^2, m_q^2)\end{aligned}\quad (4.17)$$

For the correction to the photon vertex, one just has to replace  $v_q$  by  $e_q$  and set  $a_q = 0$  in the previous equation; one obtains

$$\begin{aligned}\tilde{\Delta}_{ii}^\gamma &= \tilde{\Delta}_{ii} = 2(\tilde{m}_g^2 + \tilde{m}_q^2 + m_q^2) C_+ + 2\tilde{m}_g^2 C_0 + B_0(s, m_q^2, m_q^2) \\ &\quad - B_0(\tilde{m}_q^2, \tilde{m}_g^2, m_q^2) - (\tilde{m}_q^2 - m_q^2 - \tilde{m}_g^2) B'_0(\tilde{m}_q^2, \tilde{m}_g^2, m_q^2)\end{aligned}\quad (4.18)$$

In terms of the two and three point scalar functions  $B_0$  and  $C_0$ , the function  $C_+$  in the equal mass case simplifies to

$$C_+ = -\frac{1}{s\beta_q^2} \left[ B_0(\tilde{m}_q^2, \tilde{m}_g^2, m_q^2) - B_0(s, m_q^2, m_q^2) + (m_q^2 - \tilde{m}_g^2 - \tilde{m}_q^2) C_0 \right] \quad (4.19)$$

Note that the correction to the Z-squarks vertex can be written as

$$\tilde{\Delta}_{ii}^Z = \tilde{\Delta}_{ii} + \tilde{\delta}_{ii} \quad , \quad \tilde{\delta}_{ii} = \mp \frac{4a_q/v_q}{1 \pm a_q/v_q} m_q^2 C_+ \quad (4.20)$$

which exhibits the fact that for the superpartners of the light quarks, where one can set  $m_q = 0$ , one would have  $\tilde{\Delta}_{ii}^Z = \tilde{\Delta}_{ii}^\gamma = \tilde{\Delta}_{ii}$ .

## 5. Numerical results and discussions

In this section we will discuss the magnitude of these QCD corrections, restricting ourselves to the case of vanishing mixing angle [and hence, to the case of degenerate final state squarks] for which the numerical analysis is simpler.

First of all, Fig. 2 shows the magnitude of the QCD correction factor  $\Delta_{ii}$  due to virtual gluon exchange and real gluon emission, as a function of the velocity of the final squarks,  $\beta_q$ . As previously mentioned,  $\Delta_{ii}$  rapidly increases from the value  $\Delta_{ii} = 3$  for massless squarks (i.e.  $\beta_q = 1$ ) to reach an infinite value near the production threshold ( $\beta_q = 0$ ). Close to the latter value, perturbation theory is no more reliable and non-perturbative effects have to be taken into account.

In Fig. 3 and Fig. 4, we display the QCD correction factor  $\tilde{\Delta}_{ii}$  due to quark-gluino exchange as a function of the squark masses and for two center of mass energy values:  $\sqrt{s} = M_Z$  (Fig. 3) and  $\sqrt{s} = 500$  GeV (Fig. 4). While for the SUSY partners of light quarks, only one type of correction  $\tilde{\Delta}_{ii}$  (in Figs. 3a and 4a) is present, three types of corrections are needed for the scalar partners of the top quark:  $\tilde{\Delta}_{ii}^\gamma$  (in Figs. 3b and 4b) for photon exchange and  $\tilde{\Delta}_{ii}^Z$  for  $Z$  boson exchange and for both the left-handed and right-handed squarks (in Figs. 3c,4c and Fig. 3d,4d respectively).

As representative values of the gluino mass, we have chosen  $\tilde{m}_g = 5$  GeV, 100 GeV and 250 GeV for LEP energies and  $\tilde{m}_g = 5$  GeV, 100 GeV and 500 GeV at  $\sqrt{s} = 500$  GeV. We have allowed for the possibility that the gluinos might be very light,  $\tilde{m}_g \sim 5$  GeV. Indeed, present experimental data do not exclude this scenario and a recent analysis [18] shows that gluinos with masses in the 3–5 GeV range are still allowed<sup>1</sup>. In this case, the bounds on squark masses derived from searches for events with a large missing transverse momentum at hadron colliders [6] might be invalidated<sup>2</sup>, and thus, the only valid bounds on these masses would come from the negative searches of squark pairs in  $Z$  decays [7]. These bounds, in fact, will possibly be altered by the inclusion of the QCD corrections that we computed here, and this motivates our discussion of these contributions for LEP100 energies.

At LEP100, the QCD correction factors due to the contributions of quark-gluino loops are displayed in Fig. 3a to 3d for three values of  $\tilde{m}_g = 5$  GeV, 100 GeV and 250 GeV. They are practically constant and rather small,  $|\tilde{\Delta}_{ii}^V| < 1$ , except for the scalar partners of light quarks and for  $\tilde{m}_g = 5$  GeV, in which case  $\tilde{\Delta}_{ii}^\gamma$  varies from  $-4$  for  $\tilde{m}_q \sim 10$  GeV to  $-1.2$  near the production threshold. The reason is that for large internal particle masses, as is the case at this energy for the other two values of  $\tilde{m}_g$  and for the top quark for which we took a mass of  $m_t = 175$  GeV [20], the correction is proportional to the inverse of the mass squared; this ensure the proper decoupling of the amplitude in this limit.

<sup>1</sup>Note that, even this window would be sufficient to allow for a substantial modification of the running of the strong coupling constant [19] which is the original motivation for the renewed interest in this scenario.

<sup>2</sup>This is because of the fact that squarks will dominantly decay into light gluinos, which loose a very large fraction of their energy in QCD radiation before they decay [18], therefore leading to a soft missing transverse momentum spectrum.

For the production of squark pairs at a future high-energy  $e^+e^-$  collider with a center of mass energy of  $\sqrt{s} = 500$  GeV, the QCD correction factors are displayed in Fig. 4a to 4d for three values of  $\tilde{m}_q = 5$  GeV, 100 GeV and 500 GeV. These factors are larger than in the previous case, especially for the scalar partners of top quarks. This is due to the fact that the top mass [as well as a gluino mass of 100 GeV] is no more much larger than the beam energy and the contributions do not decouple yet. However, the corrections are still relatively small except in the light gluino window, and in some cases for gluino masses of the order of 100 GeV. Note that the dips in some of the curves correspond to the opening of the  $\tilde{q} \rightarrow q + \tilde{g}$  channel.

The QCD corrections to the cross section can be readily obtained by replacing in eq. (2.9), the bare couplings  $e_q$  and  $v_{\tilde{q}_i}$  with their renormalized values of eqs. (4.16–4.18) [to include the corrections originating from quark–gluino loops] and multiplying the bare cross section by a factor  $(1 + 4\alpha_S/(3\pi)\Delta_{ii})$  as in eq. (3.1) [to include the standard gluonic corrections]. Writing as in eq. (4.20),  $\tilde{\Delta}_{ii}^Z = \Delta_{ii} + \tilde{\delta}_{ii}$ , one obtains for the QCD corrected cross section normalized to the Born term

$$\Delta\sigma \equiv \frac{\sigma(e^+e^- \rightarrow \tilde{q}_i\tilde{q}_i)}{\sigma^B(e^+e^- \rightarrow \tilde{q}_i\tilde{q}_i)} - 1 = \frac{4\alpha_S}{3\pi} \left[ \Delta_{ii} + \tilde{\Delta}_{ii} + \frac{1}{2}\tilde{\delta}_{ii}\delta\sigma_{ii} \right] \quad (5.1)$$

with

$$\begin{aligned} \delta\sigma_{ii} = & \left[ -\frac{e_q v_e v_{q_i}}{16c_W^2 s_W^2} \frac{s}{s - M_Z^2} + \frac{(a_e^2 + v_e^2)v_{q_i}^2}{128s_W^4 c_W^4} \frac{s^2}{(s - M_Z^2)^2} \right] \\ & \times \left[ e_q^2 - \frac{e_q v_e v_{q_i}}{16c_W^2 s_W^2} \frac{s}{s - M_Z^2} + \frac{(a_e^2 + v_e^2)v_{q_i}^2}{256s_W^4 c_W^4} \frac{s^2}{(s - M_Z^2)^2} \right]^{-1} \end{aligned} \quad (5.2)$$

On the  $Z$  resonance, one can neglect the photon exchange and the interference between  $\gamma$  and  $Z$  exchanges, and the expression of  $\Delta\sigma$  simplifies to

$$\Delta\sigma \equiv \frac{\sigma(e^+e^- \rightarrow Z \rightarrow \tilde{q}_i\tilde{q}_i)}{\sigma^B(e^+e^- \rightarrow Z \rightarrow \tilde{q}_i\tilde{q}_i)} - 1 = \frac{4\alpha_S}{3\pi} (\Delta_{ii} + \tilde{\Delta}_{ii}^Z) \quad (5.3)$$

In the case of the SUSY partners of light quarks,  $\tilde{\delta}_{ii} = 0$  and, independently of the center of mass energy, one simply has

$$\Delta\sigma \equiv \frac{\sigma(e^+e^- \rightarrow \tilde{q}_i\tilde{q}_i)}{\sigma^B(e^+e^- \rightarrow \tilde{q}_i\tilde{q}_i)} - 1 = \frac{4\alpha_S}{3\pi} (\Delta_{ii} + \tilde{\Delta}_{ii}) \quad (5.4)$$

The deviation from unity of the QCD corrected cross section normalized to the Born cross section as a function of the squark masses and for the previous choices of the gluino masses is displayed in Fig. 5 and Fig. 6 for center of mass energies of respectively  $\sqrt{s} = M_Z$  and  $\sqrt{s} = 500$  GeV. In these figures, we have used for the strong coupling constant the value  $\alpha_S(M_Z^2) \simeq 0.12$  as determined from various measurements in  $Z$  decays [21]; at an energy of 500 GeV, the coupling will run down to  $\alpha_S \sim 0.11$ .

As one might expect from the previous discussion, the largest part of the QCD corrections is due to the standard gluonic corrections. The effect of the gluino-quark loops at LEP energies is important only in the case of the partners of light quarks when the gluino is very light, especially for small squark masses where the correction can even flip sign. At 500 GeV, the effect of gluino masses of the order of 100 GeV is also significant and in general, reduces the size of the QCD correction.

For large values of the gluino mass, the quark–gluino contribution decouples and only the “standard” gluonic contributions are left. In this case, even for squark masses very small compared to the center of mass energy of the collider, the QCD corrections enhance the cross section by more than 15%. The correction increases with the squark mass, and already for  $\beta_q = 0.5$ , one has a correction of more than 50%. These corrections are therefore much larger than the ones affecting the pair production in  $e^+e^-$  collisions of spin 1/2 particles with the same mass [22].

## 6. Summary

In this paper, we have calculated the QCD radiative corrections to the production of the supersymmetric partners of quarks in  $e^+e^-$  collisions. We have taken into account the mixing between left- and right-handed scalar quarks, and this led us to treat the case where the two final state particles have different masses. We included both the standard gluonic corrections consisting of virtual gluon exchange and real gluon emission (which, in the limiting case where the scalar particles are degenerate in mass, have been calculated long time ago by Schwinger for scalar QED) and also the genuine SUSY QCD corrections due to quark–gluino loops (which do not appear in scalar QED). For both types of corrections, complete analytical expressions were given in the general case.

We have then discussed the magnitude of these QCD corrections in the case of vanishing mixing angle. We have shown that the corrections due to quark–gluino loops are important only when the gluinos have relatively small masses, and in this case, particularly for the production of the partners of light quarks. For large gluino masses, these corrections decouple as they should, and only the contributions due to gluon exchange and real gluon emission are left in this limit. The latter corrections are very important since, even for massless squarks where they are minimal, they enhance the cross section by more than 15%, four times as much as the QCD corrections affecting the production of spin 1/2 massless quarks.

**Acknowledgements:** We thank M. Drees and P. Ouellette for discussions.

## Appendix: Scalar Loop Integrals

In this Appendix we collect expressions that allow to evaluate the loop functions that appear in section 4. The scalar one, two and three point functions,  $A_0$ ,  $B_0$  and  $C_0$  are defined as

$$\begin{aligned}
A_0(m_0) &= \frac{(2\pi\mu)^{n-4}}{i\pi^2} \int \frac{d^n k}{k^2 - m_0^2 + i\epsilon} \\
B_0(s, m_1, m_2) &= \frac{(2\pi\mu)^{n-4}}{i\pi^2} \int \frac{d^n k}{(k^2 - m_1^2 + i\epsilon)[(k - q)^2 - m_2^2 + i\epsilon]} \\
C_0(m_1, m_2, m_3) &= \frac{(2\pi\mu)^{n-4}}{i\pi^2} \int \frac{d^n k}{[(k - p_1)^2 - m_1^2 + i\epsilon][(k - p_2)^2 - m_2^2 + i\epsilon](k^2 - m_3^2 + i\epsilon)}
\end{aligned} \tag{A.1}$$

Here  $n$  is the space–time dimension and  $\mu$  the renormalisation scale. After integration over the internal momentum  $k$ , the function  $A_0$  is given by [ $\gamma_E$  is Euler’s constant]:

$$A_0(m_0) = m_0^2 [1 + \Delta_0] \quad , \quad \Delta_i = \frac{2}{4 - n} - \gamma_E + \log(4\pi) + \log \frac{\mu^2}{m_i^2} \tag{A.2}$$

The function  $B_0$  and its derivative with respect to  $s$ ,  $B'_0$ , are given by

$$\begin{aligned}
B_0(s, m_1, m_2) &= \frac{1}{2}(\Delta_1 + \Delta_2) + 2 + \frac{m_1^2 - m_2^2}{2s} \log \frac{m_2^2}{m_1^2} + \frac{x_+ - x_-}{4s} \log \frac{x_-}{x_+} \\
B'_0(s, m_1, m_2) &= -\frac{1}{2s} \left[ 2 + \frac{m_2^2 - m_1^2}{s} \log \frac{m_1^2}{m_2^2} + \frac{2(m_1^2 - m_2^2)^2 - s(m_1^2 + m_2^2)}{s(x_+ - x_-)} \log \frac{x_-}{x_+} \right]
\end{aligned} \tag{A.3}$$

with

$$x_{\pm} = s - m_1^2 - m_2^2 \pm \sqrt{s^2 - 2s(m_1^2 + m_2^2) + (m_1^2 - m_2^2)^2} \tag{A.4}$$

Note that the  $x_{\pm}$  can be complex; however we have ignored the imaginary parts of  $B_0$  and  $B'_0$  since they are not relevant for us: to next–to–leading order we are only interested in the interference between the (real) tree–level and one–loop amplitudes.

We also need the three point scalar function  $C_0$  which can be written in integral form as

$$C_0(\tilde{m}_1^2, \tilde{m}_2^2, s, m_1, m_2, m_3) = - \int_0^1 dy \int_0^y dx [ay^2 + bx^2 + cxy + dy + ex + f]^{-1} \tag{A.5}$$

where

$$a = m_q^2, \quad b = s, \quad c = -s, \quad d = m_2^2 - m_3^2 - m_q^2, \quad e = m_1^2 - m_2^2, \quad f = m_3^2 - i\epsilon \tag{A.6}$$

The full analytical expression of  $C_0$  in terms of Spence functions can be found in Ref. [14].

## References

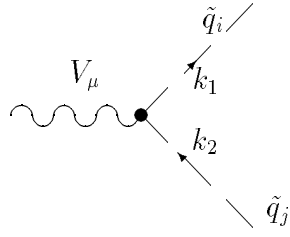
- [1] H.E. Haber and G.L. Kane, Phys. Rep. 117 (1985) 75.
- [2] H.P. Nilles, Phys. Rep. 110 (1984) 1;  
P. Nath, R. Arnowitt and A. Chamseddine, “Applied N=1 Supergravity”, ITCP Series in Theoretical Physics, World Scientific, Singapore 1984;  
X.R. Tata, in Proceedings of the “Mt Sorak Symposium on the Standard Model and Beyond”, Mt Sorak, Korea, 1990
- [3] E. Witten, Nucl. Phys. B188 (1981) 513;  
N. Sakai, Z. Phys. C11 (1981) 153;  
S. Dimopoulos and H. Georgi, Nucl. Phys. B193 (1981) 150.
- [4] U. Amaldi, W. de Boer and H. Fürstenau, Phys. Lett. B260 (1991) 447;  
P. Langacker and M. Luo, Phys. Rev. D44 (1991) 817;  
J. Ellis, S. Kelley and D.V. Nanopoulos, Phys. Lett. B260 (1991) 131.
- [5] See e.g. M. Kamionkowski, “Supersymmetric Dark Matter”, in the Proceedings of the Workshop on High Energy Astrophysics, Honolulu, Hawaii, March 1992, edited by J.G. Learned and X.R. Tata.
- [6] CDF Collab., F. Abe et al., Phys. Rev. Lett. 69 (1992) 3439.
- [7] M. Davier, in Proceedings of the Joint International Lepton–Photon Symposium and European Conference on High Energy Physics, Geneva, Switzerland, 1991, edited by S. Hegarty, K. Potter and E. Quereigh (World Scientific, Singapore, 1992).
- [8] W. Beenakker, R. Höpker, M. Spira and P. Zerwas, Report DESY 94–212; hep-ph 9412272.
- [9] J. Schwinger, Particles, Sources and Fields, Vol. II, Addison–Wesley, New York, 1973.
- [10] M. Drees and K. Hikasa, Phys. Lett. B252 (1990) 127.
- [11] J. Ellis and S. Rudaz, Phys. Lett. B128 (1983) 248.
- [12] K. Hikasa and M. Kobayashi, Phys. Rev. D36 (1987) 724.
- [13] G. Passarino and M. Veltman, Nucl. Phys. B160 (1979) 151.
- [14] G. ’t Hooft and M. Veltman, Nucl. Phys. B153 (1979) 365.
- [15] A. Denner, Fortsch. Phys. 41 (1993) 307.
- [16] K. Hagiwara et al., Nucl. Phys. B344 (1990) 1;  
I. Bigi, V. Fadin and V. Khoze, Nucl. Phys. B377 (1992) 461.



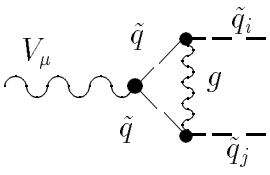
- [17] A. Djouadi, M. Drees and H. König, Phys. Rev. D48 (1993) 3081.
- [18] G. R. Farrar, Preprint RU-94-35 (August 1994); it also appeared as a hep-ph 9407401.
- [19] L. Clavelli, Phys. Rev. D46, 2112 (1992);  
L. Clavelli, P.W. Coulter and K. Yuan, Phys. Rev. D47 (1993) 1973;  
M. Jezabek and J.H. Kühn, Phys. Lett. B301 (1993) 121;  
J. Ellis, D.V. Nanopoulos and D.A. Ross, Phys. Lett. B305 (1993) 375;  
L. Clavelli and P.W. Coulter, Alabama Univ. report UAHEP-941 (1994).
- [20] CDF Collab., F. Abe et al., Preprint Fermilab-Pub-94/116/E (May 1994).
- [21] For a recent compilation of LEP results on  $\alpha_S$  see, S. Bethke, Report PITHA-94-29 (August 1994).
- [22] J. Jerzak, E. Laermann and P. M. Zerwas, Phys. Rev. D25 (1980) 1218;  
R. Reinders, Rubinstein and Yazaki, Phys. Rep. C127 (1985) 1;  
G. Grunberg, Y.J. Ng and S.H.H. Tye, al.; Phys. Rev. D21 (1980) 62;  
A. Djouadi, Z. Physik C39 (1988) 561;  
A. Djouadi, J. H. Kühn and P. M. Zerwas, Z. Physik C46 (1990) 411.

## Figure Captions

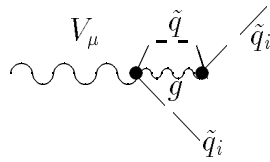
- Fig. 1 Feynman diagrams for the QCD corrections to the decay of a gauge boson into squark pairs: tree-level diagram (1a); vertex (1b) and self-energy (1c) standard gluonic corrections and real gluon emission (1d) ; vertex (1e) and self-energy (1f) corrections due to quark-gluino loops.
- Fig. 2 The QCD correction factor  $\Delta_{ii}$  due to virtual gluon exchange and real gluon emission as a function of the velocity of the final squarks  $\beta$ . The two squarks are assumed to be degenerate in mass.
- Fig. 3 The QCD correction factors due to virtual quark-gluino exchange as a function of the squark mass and for selected values of the gluino mass at  $\sqrt{s} = M_Z$ :  $\tilde{\Delta}_{ii}$  for the partners of light quarks (3a),  $\tilde{\Delta}_{ii}^\gamma$  for degenerate stop squarks (3b) and  $\tilde{\Delta}_{ii}^Z$  for the left-handed (3c) and right-handed stop squarks (3d). The full line is for  $\tilde{m}_g = 250$  GeV, the dashed line for  $\tilde{m}_g = 100$  GeV and the dot-dashed line for  $\tilde{m}_g = 5$  GeV.
- Fig. 4 The QCD correction factors due to virtual quark-gluino exchange as a function of the squark mass and for selected values of the gluino mass at  $\sqrt{s} = 500$  GeV:  $\tilde{\Delta}_{ii}$  for the partners of light quarks (4a),  $\tilde{\Delta}_{ii}^\gamma$  for degenerate stop squarks (4b) and  $\tilde{\Delta}_{ii}^Z$  for the left-handed (4c) and right-handed stop squarks (4d). The full line is for  $\tilde{m}_g = 500$  GeV, the dashed line is for  $\tilde{m}_g = 100$  GeV and the dot-dashed line for  $\tilde{m}_g = 5$  GeV.
- Fig. 5 The deviation from unity of the fully QCD corrected cross section normalized to the Born cross section as a function of the squark masses and for selected values of the gluino mass at  $\sqrt{s} = M_Z$ : for the partners of light quarks (5a), and for the left-handed (5b) and right-handed stop squarks (5c). The full line is for  $\tilde{m}_g = 250$  GeV, the dashed line for  $\tilde{m}_g = 100$  GeV and the dot-dashed line for  $\tilde{m}_g = 5$  GeV.
- Fig. 6 The deviation from unity of the fully QCD corrected cross section normalized to the Born cross section as a function of the squark masses and for selected values of the gluino mass at  $\sqrt{s} = 500$  GeV: for the partners of light quarks (6a), and for the left-handed (6b) and right-handed stop squarks (6c). The full line is for  $\tilde{m}_g = 500$  GeV, the dashed line is for  $\tilde{m}_g = 100$  GeV and the dot-dashed line for  $\tilde{m}_g = 5$  GeV.



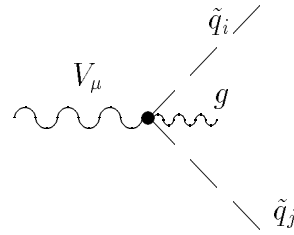
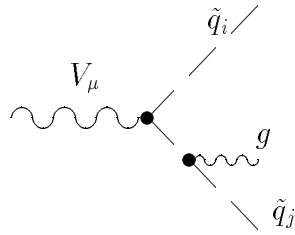
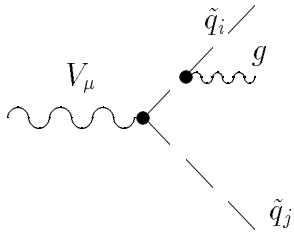
1.a



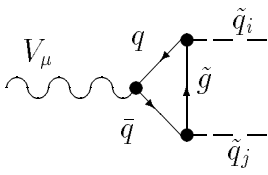
1.b



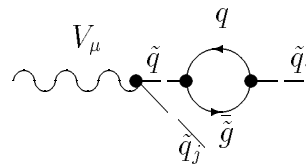
1.c



1.d



1.e



1.f

Figure 1

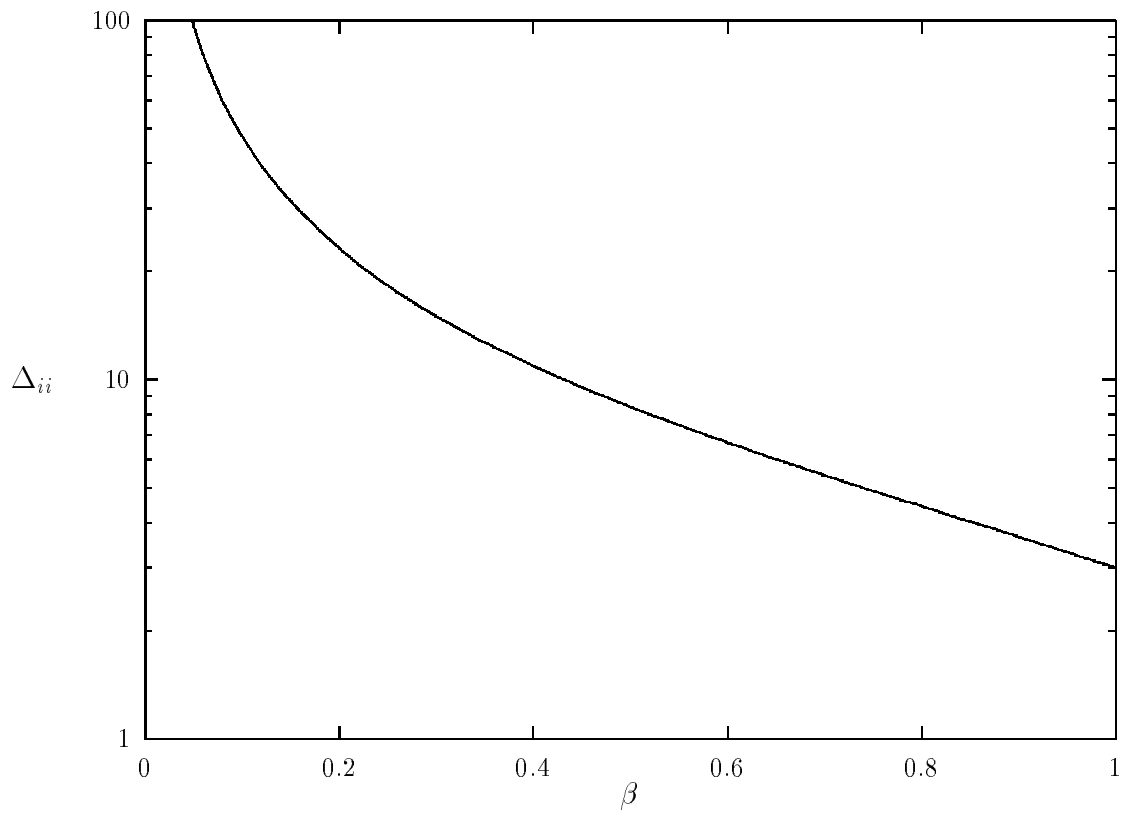


**Figure 2**

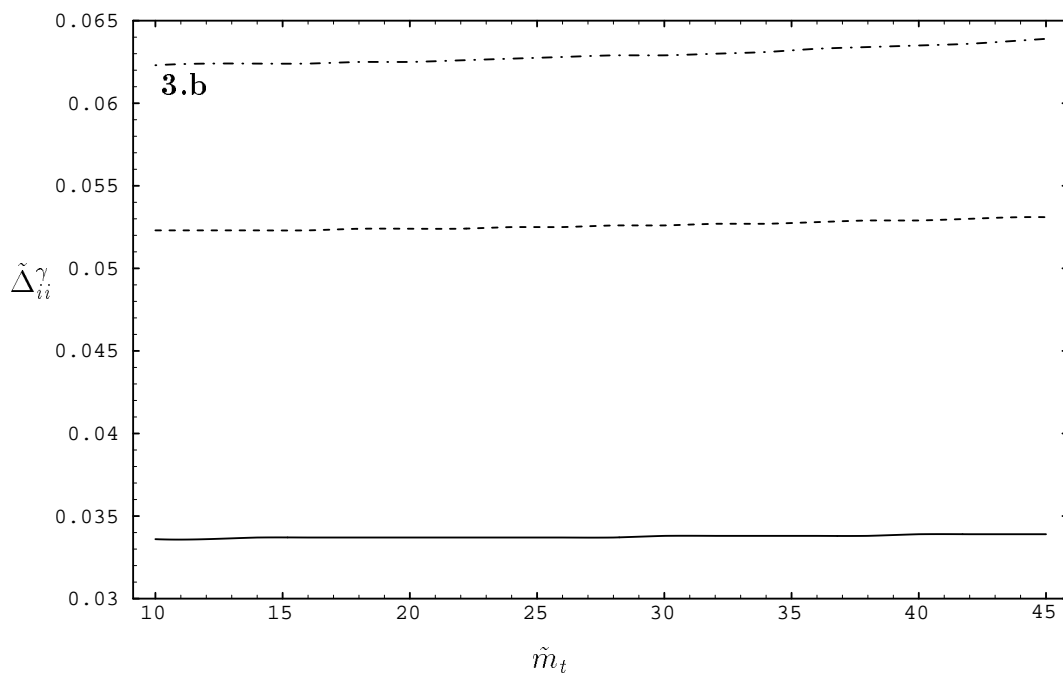
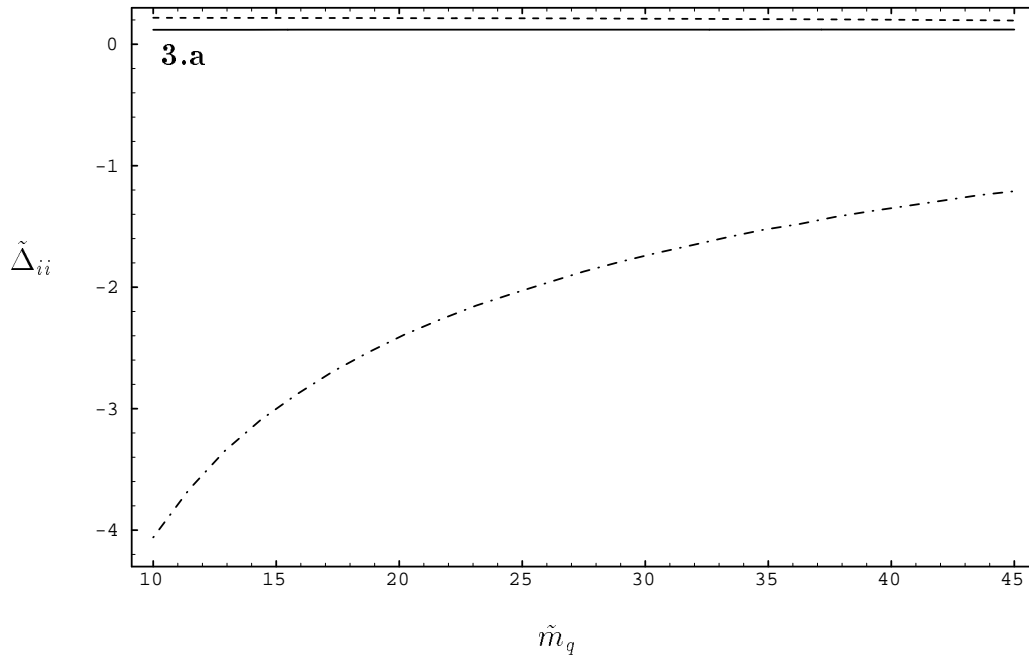


**Figure 3**

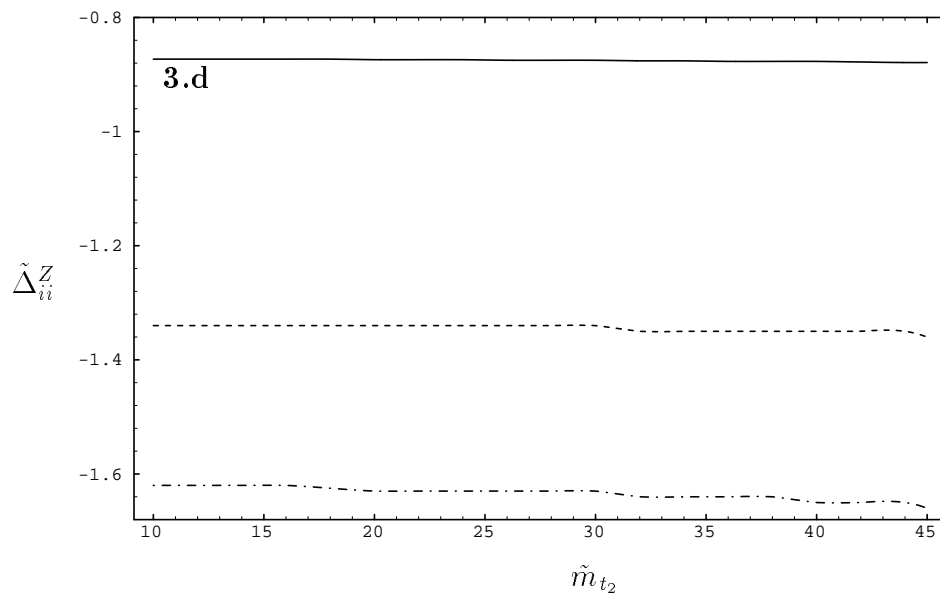
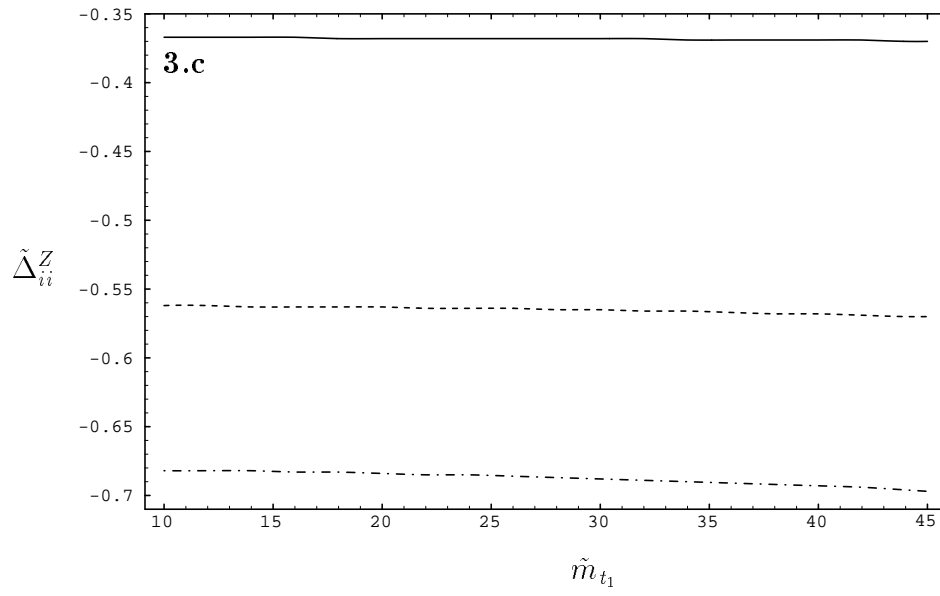
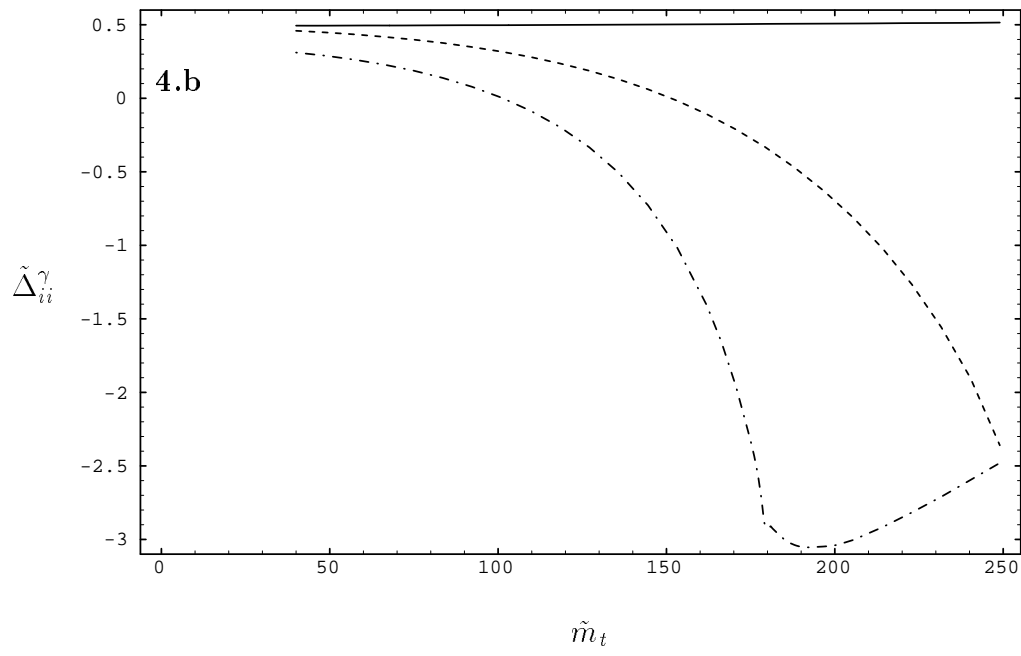
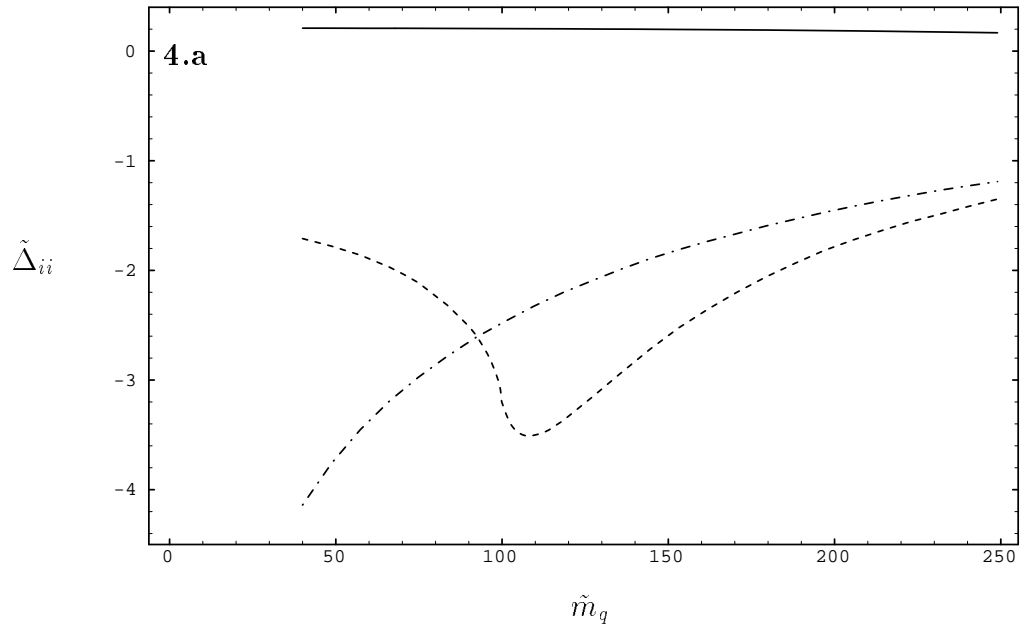


Figure 3 (cont.)



**Figure 4**

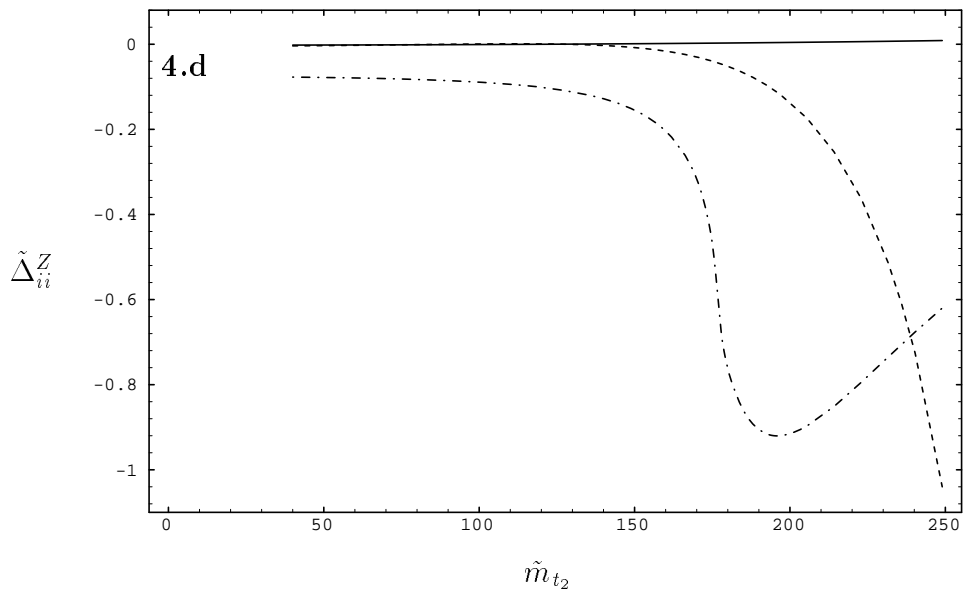
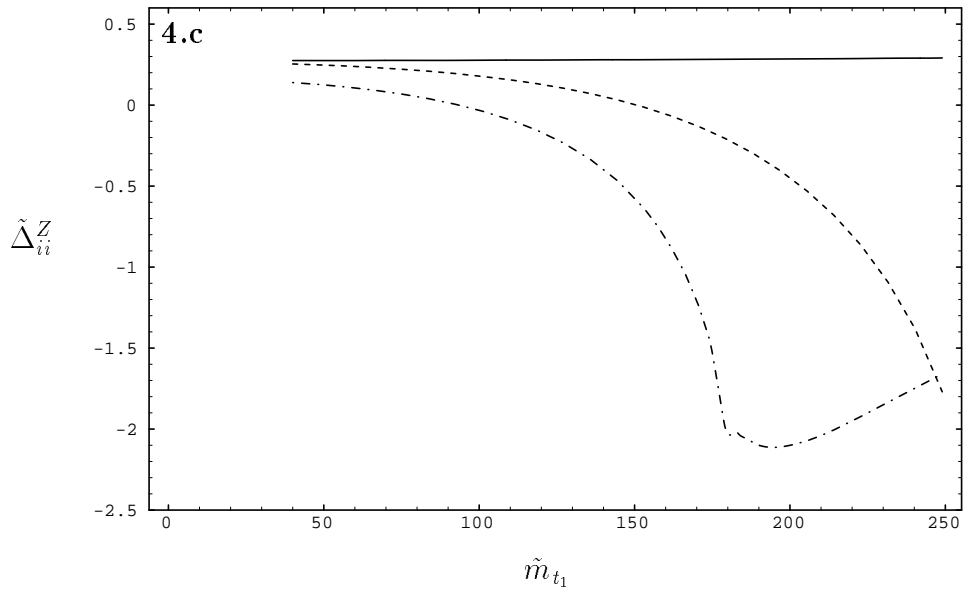


Figure 4 (cont.)



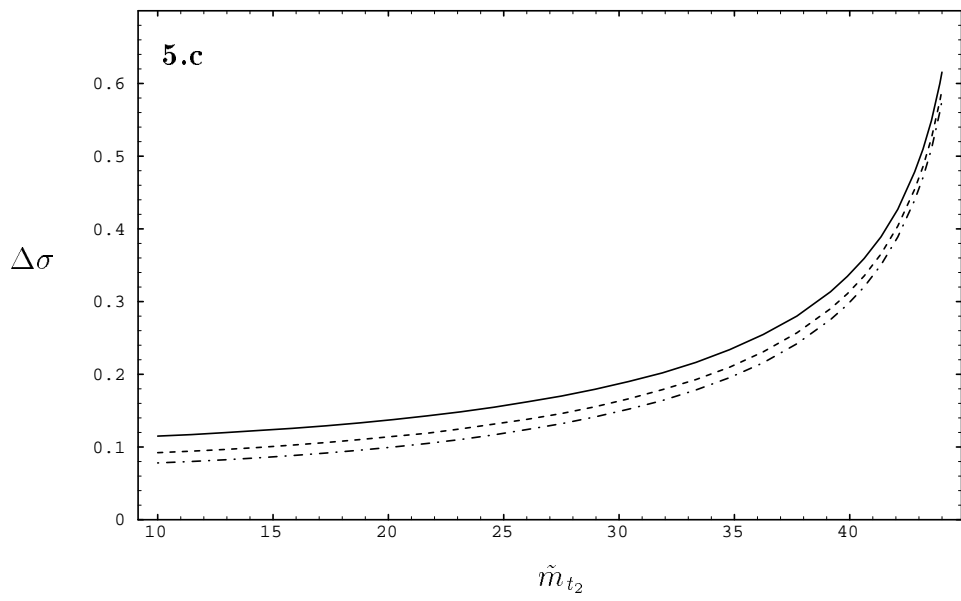
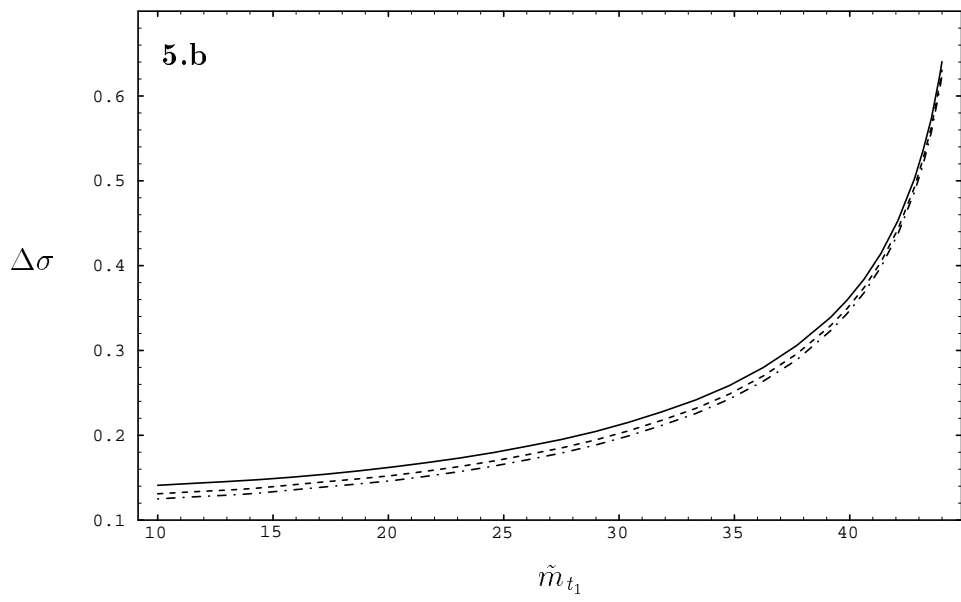
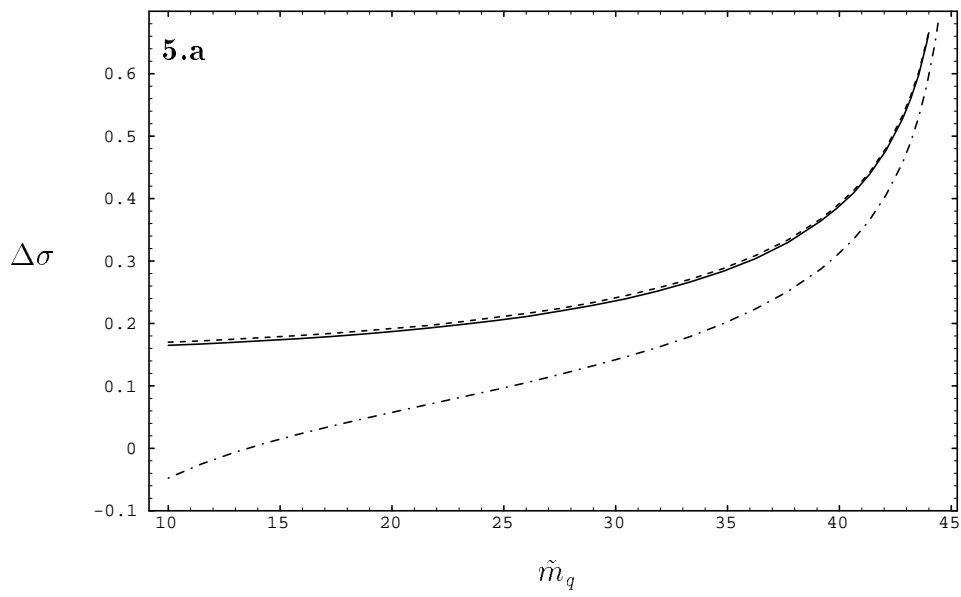
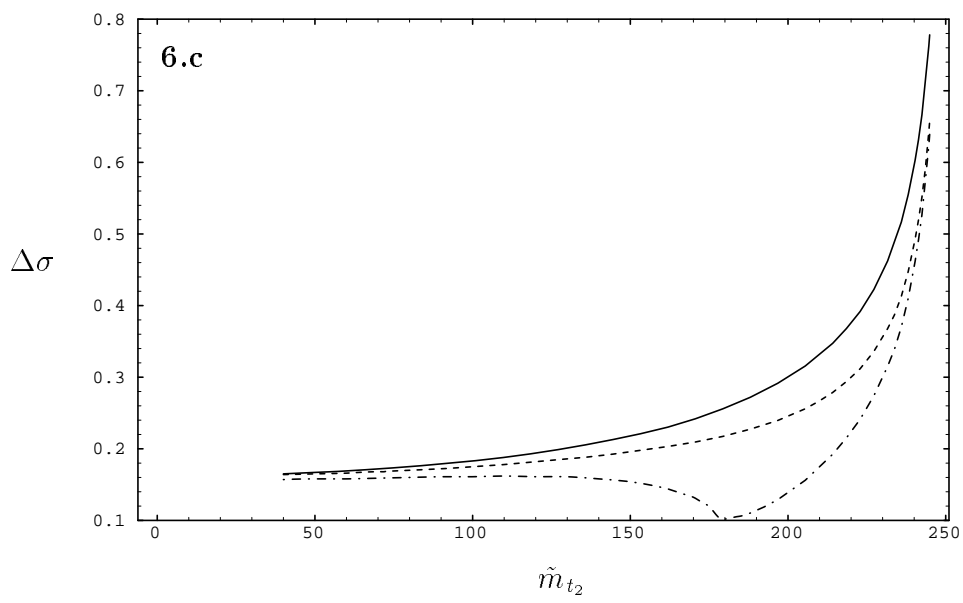
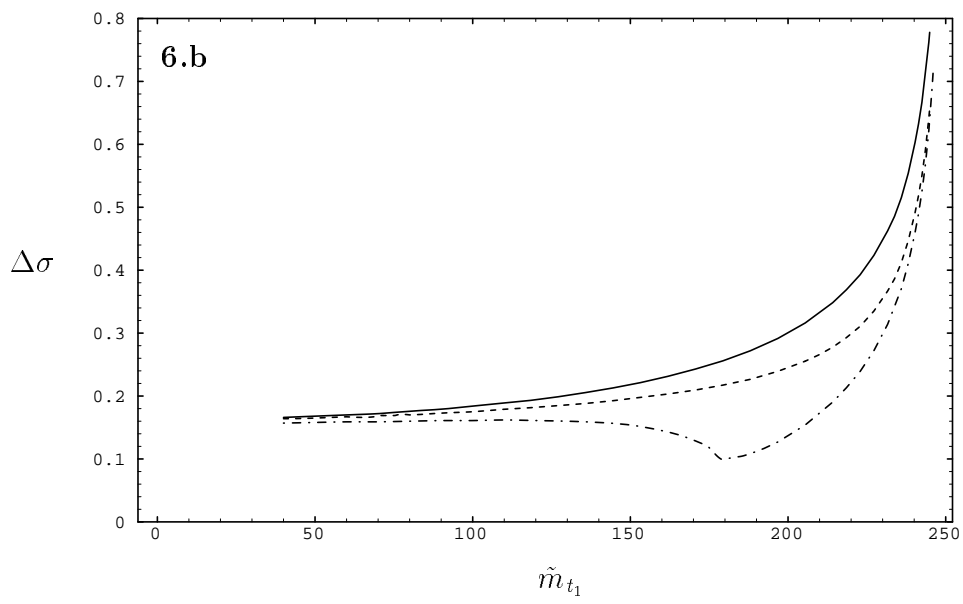
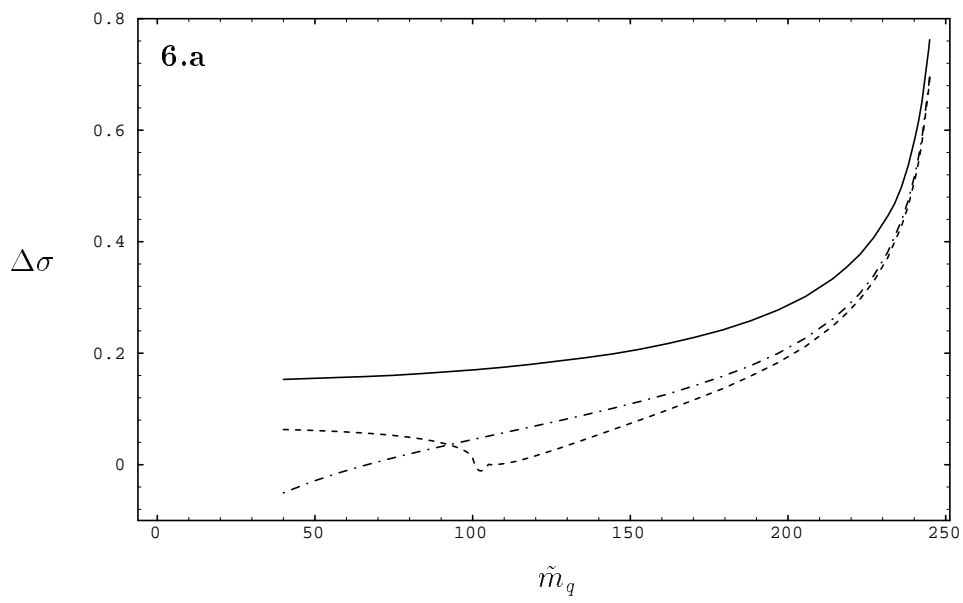


Figure 5



**Figure 6**

This figure "fig1-1.png" is available in "png" format from:

<http://arxiv.org/ps/hep-ph/9412382v2>

This figure "fig1-2.png" is available in "png" format from:

<http://arxiv.org/ps/hep-ph/9412382v2>

This figure "fig1-3.png" is available in "png" format from:

<http://arxiv.org/ps/hep-ph/9412382v2>

This figure "fig1-4.png" is available in "png" format from:

<http://arxiv.org/ps/hep-ph/9412382v2>

This figure "fig1-5.png" is available in "png" format from:

<http://arxiv.org/ps/hep-ph/9412382v2>

This figure "fig1-6.png" is available in "png" format from:

<http://arxiv.org/ps/hep-ph/9412382v2>



This figure "fig1-7.png" is available in "png" format from:

<http://arxiv.org/ps/hep-ph/9412382v2>

This figure "fig1-8.png" is available in "png" format from:

<http://arxiv.org/ps/hep-ph/9412382v2>